

Large Structure Rearrangement of Colicin Ia Channel Domain after Membrane Binding from 2D ^{13}C Spin Diffusion NMR

Wenbin Luo, Xiaolan Yao,[†] and Mei Hong*

Contribution from the Department of Chemistry, Iowa State University, Ames, Iowa 50011

Received November 5, 2004; E-mail: mhong@iastate.edu

Abstract: One of the main mechanisms of membrane protein folding is by spontaneous insertion into the lipid bilayer from the aqueous environment. The bacterial toxin, colicin Ia, is one such protein. To shed light on the conformational changes involved in this dramatic transfer from the polar to the hydrophobic milieu, we carried out 2D magic-angle spinning ^{13}C NMR experiments on the water-soluble and membrane-bound states of the channel-forming domain of colicin Ia. Proton-driven ^{13}C spin diffusion spectra of selectively ^{13}C -labeled protein show unequivocal attenuation of cross-peaks after membrane binding. This attenuation can be assigned to distance increases but not reduction of the diffusion coefficient. Analysis of the statistics of the interhelical and intrahelical ^{13}C – ^{13}C distances in the soluble protein structure indicates that the observed cross-peak reduction is well correlated with a high percentage of short interhelical contacts in the soluble protein. This suggests that colicin Ia channel domain becomes open and extended upon membrane binding, thus lengthening interhelical distances. In comparison, cross-peaks with similar intensities between the two states are dominated by intrahelical contacts in the soluble state. This suggests that the membrane-bound structure of colicin Ia channel domain may be described as a “molten globule”, in which the helical secondary structure is retained while the tertiary structure is unfolded. This study demonstrates that ^{13}C spin diffusion NMR is a valuable tool for obtaining qualitative long-range distance constraints on membrane protein folding.

Introduction

The determination of the 3D structure of solid proteins by NMR has made dramatic progress in the past few years due to advances in the preparation of ordered and microcrystalline proteins,¹ multidimensional resonance assignment techniques,^{2–5} and distance⁶ and torsion angle^{7,8} determination methods for uniformly ^{13}C , ^{15}N -labeled proteins.^{9,10} Short-range distances (<5 Å) that restrain both backbone and local side chain conformations can now be measured accurately. However, long-range distances ($\gg 5$ Å) are still difficult to determine, calling for development of methods to measure dipolar couplings between spins with high gyromagnetic ratios.^{11,12}

In fortunate cases, information on very long distances may be deduced unambiguously using semiquantitative approaches such as spin diffusion. We show here that a classical 2D ^{13}C correlation technique, ^1H -driven ^{13}C spin diffusion (PDSD), yields fresh new insight into the 3D fold of a large membrane protein, the channel-forming domain of colicin Ia (25,082 Da). A bacterial toxin, colicin Ia exerts its toxic effect by spontaneously inserting into the inner membrane of sensitive bacteria cells from the aqueous environment and opening a voltage-gated channel that depletes the membrane potential of the cell.¹³ How the protein changes its structure to adapt to both the polar and hydrophobic milieu is a fascinating and fundamental biophysical problem. The water-soluble structure of colicin Ia has been determined by X-ray crystallography¹⁴ and shows the channel domain to be a compact 10 α -helix globule. However, the high-resolution structure of the membrane-bound (MB) state is still unknown. Our earlier ^{13}C chemical shift analysis indicated that the protein backbone largely preserves its α -helical conformation upon membrane binding.¹⁵ Various biophysical measurements indicated that homologous colicins adopt an open conformation upon membrane binding, with a hydrophobic helical hairpin well embedded in the lipid bilayer.^{16–23} A schematic of this large

[†] Current address: Department of Biochemistry, University of Texas Southwestern Medical Center at Dallas, 5323 Harry Hines Boulevard, Dallas, TX 75390-9038.

- (1) Martin, R. W.; Zilm, K. W. *J. Magn. Reson.* **2003**, *165*, 162–174.
- (2) Pauli, J.; Baldus, M.; vanRossum, B.; Groot, H. d.; Oschkinat, H. *ChemBioChem* **2001**, *2*, 272–281.
- (3) McDermott, A. E.; Polenova, T.; Bockmann, A.; Zilm, K. W.; Paulsen, E. K.; Martin, R. W.; Montellione, G. T. *J. Biomol. NMR* **2000**, *16*, 209–219.
- (4) Hong, M. *J. Biomol. NMR* **1999**, *15*, 1–14.
- (5) Detken, A.; Hardy, E. H.; Ernst, M.; Kainosho, M.; Kawakami, T.; Aimoto, S.; Meier, B. H. *J. Biomol. NMR* **2001**, *20*, 203–221.
- (6) Jaroniec, C. P.; Filip, C.; Griffin, R. G. *J. Am. Chem. Soc.* **2002**, *124*, 10728–10742.
- (7) Rienstra, C. M.; Hohwy, M.; Mueller, L. J.; Jaroniec, C. P.; Reif, B.; Griffin, R. G. *J. Am. Chem. Soc.* **2002**, *124*, 11908–11922.
- (8) Antzutkin, O. N. In *Solid-state NMR spectroscopy principles and applications*; Duer, M. J., Ed.; Blackwell Sciences: Oxford, 2002; pp 280–390.
- (9) Castellani, F.; vanRossum, B.; Diehl, A.; Schubert, M.; Rehbein, K.; Oschkinat, H. *Nature* **2002**, *420*, 98–102.
- (10) Jaroniec, C. P.; MacPhee, C. E.; Bajaj, V. S.; McMahon, M. T.; Dobson, C. M.; Griffin, R. G. *Proc. Natl. Acad. Sci. U.S.A.* **2004**, *101*, 711–716.
- (11) Schmidt-Rohr, K.; Hong, M. *J. Am. Chem. Soc.* **2003**, *125*, 5648–5649.

- (12) Wi, S.; Sinha, N.; Hong, M. *J. Am. Chem. Soc.* **2004**, *126*, 12754–12755.
- (13) Cramer, W. A.; Heymann, J. B.; Schendel, S. L.; Deriy, B. N.; Cohen, F. S.; Elkins, P. A.; Stauffacher, C. V. *Annu. Rev. Biophys. Biomol. Struct.* **1995**, *24*, 611–641.
- (14) Wiener, M.; Freymann, D.; Ghosh, P.; Stroud, R. M. *Nature* **1997**, *385*, 461–464.
- (15) Huster, D.; Yao, X.; Jakes, K.; Hong, M. *Biochim. Biophys. Acta* **2002**, *1561*, 159–170.

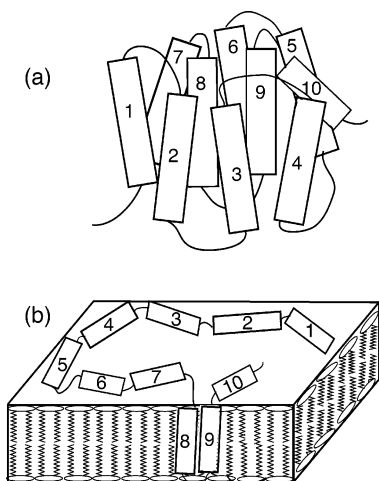


Figure 1. Protein refolding from a globular structure with hydrophobic residues inside (a) to an open topology with the hydrophobic residues exposed to the lipid molecules (b).

conformational change is shown in Figure 1. However, to date, no direct distance measurements for the unfolding of colicin Ia channel domain has been reported.

Here we report 2D ^{13}C PDSO experiments that support an extended topology for the MB state of colicin Ia channel domain. We found that inter-residue cross-peaks are significantly attenuated in the MB protein compared to the soluble protein. Moreover, the intensity reduction is more pronounced for inter-residue cross-peaks with a high fraction of interhelical contacts in the soluble state. Given the similar secondary structure of the two states of the protein, this suggests that membrane binding lengthens the interhelical distances while retaining the intra-helical distances.

Materials and Methods

Preparation of Soluble and Membrane-Bound Colicin Ia Channel Domain. All ^{13}C - and ^{15}N -labeled compounds, including $^{15}\text{NH}_4\text{Cl}$, ^{15}N -Glu, ^{15}N -Gln, $[1,6\text{-}^{13}\text{C}]$ glucose, and $[\text{U-}^{13}\text{C}]$ glucose, were purchased from Cambridge Isotope Laboratory (Andover, MA). His₆-tagged colicin Ia channel domain was expressed from pKJ120-containing *Escherichia coli* BL21 (DE3) cells in a modified M9 medium containing appropriate isotopic labels and was purified by His-bind metal chelation resin (Novagen) as described before.^{15,24} TEASE protocol was used for isotopic labeling,²⁴ where the labeled ^{13}C and ^{15}N precursors are supplemented with 10 unlabeled amino acids from the citric acid cycle (Glu, Gln, Arg, Pro, Asn, Asp, Lys, Ile, Met, Thr). In this way, only the amino acids from the glycolysis pathway and the pentose phosphate pathway (Gly, Ser, Cys, His, Ala, Val, Leu, Trp, Phe, Tyr) are labeled. This simplifies the ^{13}C spectra and allows straightforward peak assignment to the amino acid type. The ^{13}C

precursor was either $[1,6\text{-}^{13}\text{C}]$ glucose or $[\text{U-}^{13}\text{C}]$ glucose. For the former, the labeled ^{13}C sites are Ala C β , Leu C α , C δ 1, C δ 2, Ser C β , Cys C β , Val C γ 1, C γ 2, His C δ 2, C', Phe C β , C γ , C δ 1, C δ 2, Tyr C β , C δ 1, C δ 2, C ζ , and Trp C β , C δ 2, C ϵ 1, C ϵ 2.²⁵ This sample is called 1,6-colicin. The main ^{15}N precursor was ^{15}N -ammonium chloride, supplemented with ^{15}N -Glu and ^{15}N -Gln to reduce dilution of the ^{15}N labeling level by the transamination reaction. The yield of the protein was 20–30 mg/L.

The soluble colicin sample was prepared by packing dry, lipid-free, colicin directly into a 4-mm magic-angle spinning (MAS) rotor, then hydrating it to 35% water by mass. The MB protein sample was prepared by mixing the protein solution with vesicle solutions of POPC and POPG lipid mixtures (Avanti Polar Lipids, Alabaster, AL) to achieve a protein–lipid molar ratio of 1:100. The molar ratio of neutral POPC to anionic POPG lipids was 3:7. The lipid solution, in a citrate buffer of pH 4.8 (0.3 M KCl, 10 mM citrate), was extruded across polycarbonate filter membranes of 100-nm diameter²⁶ to produce large unilamellar vesicles before protein binding. The mixed proteoliposome solution was ultracentrifuged at 150000g for 2 h using a Beckman swinging-bucket rotor (SW60 Ti) to obtain a membrane pellet. The supernatant contained less than 5% unbound protein, as measured by a photometric assay.²⁷ The membrane protein pellet was lyophilized, packed into a 4-mm MAS rotor, and hydrated to 35% water by mass.

Solid-State NMR. 2D PDSO experiments were carried out on a Bruker DSX-400 spectrometer (Karlsruhe, Germany) operating at a resonance frequency of 100.71 MHz for ^{13}C . A double-resonance MAS probe with a 4-mm spinning module was used. The ^1H radio frequency field strengths for heteronuclear TPPM decoupling²⁸ were 70 kHz. ^1H and ^{13}C 90° pulse lengths were typically 3.5 and 5.0 μs , respectively. Cross polarization (CP) contact time was 0.2–0.5 ms. Spinning speeds were 5 kHz for 1,6-colicin and 6 kHz for the partial uniformly labeled colicin (pU-colicin) to avoid rotational resonance effects.²⁹ The spectra were collected with 160–320 scans per t_1 slice, a spectral window of 20 kHz for the indirect dimension, and a maximum t_1 evolution time of 6.8 ms. The ^{13}C mixing times ranged from 50 to 500 ms. For the ^1H spin diffusion experiment, the second and third ^1H – ^{13}C CP contact time was 200 μs . The ^1H spin diffusion mixing times ranged from 150 to 350 μs .

Results and Discussion

Figure 2a,b shows the 1D ^{13}C CP-MAS spectra of the membrane-bound and soluble 1,6-colicin. The MB protein (a) does not exhibit excessively high lipid peaks due to the use of a short CP contact time, 200 μs . The most visible lipid background signal is the 32 ppm (CH₂)_n peak, which is resolved from the protein signals. Figure 2c shows the 2D INADEQUATE spectrum of the soluble pU-colicin. The ^{13}C peaks were readily assigned to amino acid types based on the characteristic chemical shifts and the connectivity pattern in the 2D spectrum. The clean suppression of the citric acid cycle amino acids was demonstrated by the weakness of the carbonyl and several side chain signals. Quantitative analysis of 1D direct-polarization spectrum (Supporting Information Figure S1) indicates that the $^{13}\text{C}'$ intensity is consistent with the predicted labeling of only His residues in the protein. If the citric acid cycle is not suppressed, a much higher $^{13}\text{C}'$ peak of twice the

- (16) Zakharov, S. D.; Lindeberg, M.; Griko, Y.; Salamon, Z.; Tollin, G.; Prendergast, F. G.; Cramer, W. A. *Proc. Natl. Acad. Sci. U.S.A.* **1998**, *95*, 4282–4287.
 (17) Lindeberg, M.; Zakharov, S. D.; Cramer, W. A. *J. Mol. Biol.* **2000**, *295*, 679–692.
 (18) Lakey, J. H.; Baty, D.; Pattus, F. *J. Mol. Biol.* **1991**, *218*, 639–653.
 (19) Shin, Y.; Levinthal, C.; Levinthal, F.; Hubbell, W. L. *Science* **1993**, *259*, 960–963.
 (20) Massotte, D.; Yamamoto, M.; Scianimanico, S.; Sorokine, O.; Dorsselaer, A. v.; Nakatani, Y.; Ourisson, G.; Pattus, F. *Biochemistry* **1993**, *32*, 13787–13794.
 (21) van der Goot, F. G.; Gonzalez-Manas, J. M.; Lakey, J. H.; Pattus, F. *Nature* **1991**, *354*, 408–410.
 (22) Huster, D.; Yao, X.; Hong, M. *J. Am. Chem. Soc.* **2002**, *124*, 874–883.
 (23) Kim, Y.; Valentine, K.; Opella, S. J.; Schendel, S. L.; Cramer, W. A. *Protein Sci.* **1998**, *7*, 342–348.
 (24) Hong, M.; Jakes, K. *J. Biomol. NMR* **1999**, *14*, 71–74.

- (25) Hong, M. *J. Magn. Reson.* **1999**, *139*, 389–401.
 (26) Hope, M. J.; Bally, M. B.; Webb, G.; Cullis, P. R. *Biochim. Biophys. Acta* **1985**, *812*, 55–65.
 (27) Smith, P. K.; Krohn, R. I.; Hermanson, G. T.; Mallia, A. K.; Gartner, F. H.; Provenzano, M. D.; Fujimoto, E. K.; Goetze, N. M.; Olson, B. J.; Klenk, D. C. *Anal. Biochem.* **1985**, *150*, 76–85.
 (28) Bennett, A. E.; Rienstra, C. M.; Auger, M.; Lakshmi, K. V.; Griffin, R. G. *J. Chem. Phys.* **1995**, *103*, 6951–6958.
 (29) Raleigh, D. P.; Levitt, M. H.; Griffin, R. G. *Chem. Phys. Lett.* **1988**, *146*, 71–76.

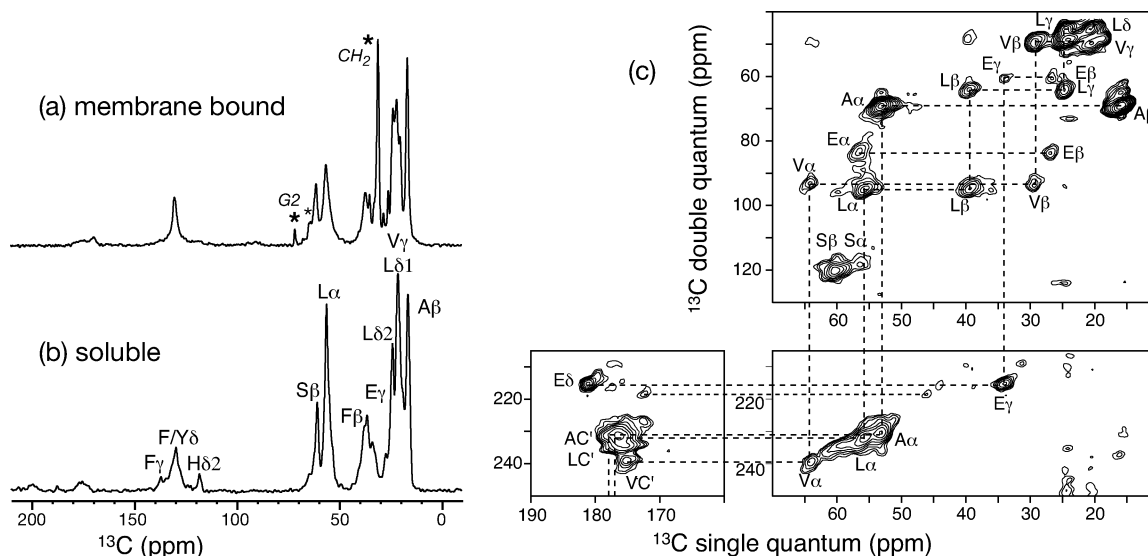


Figure 2. ^{13}C assignment of colicin Ia channel domain. (a,b) 1D ^{13}C CP-MAS spectra of 1,6-colicin in the (a) membrane-bound and (b) soluble states. Lipid peaks are indicated by asterisks. (c) 2D dipolar INADEQUATE spectrum of soluble pU-colicin.

Leu C α signal would be expected. This was not observed. For methyl-containing Thr, if scrambling occurred, its C β site (~ 67 ppm) would be labeled at a level higher than C γ (~ 20 ppm), and thus two correlation peaks would be expected in the 2D INADEQUATE spectrum. No such peaks were observed. Similarly, for the only other methyl-containing amino acid of the citric acid cycle, Ile, the lack of C $\gamma 1$ –C $\gamma 2$ correlation peaks in the 2D spectrum and the lack of a resolved C δ signal (~ 10 ppm) in the 1D spectrum rule out scrambling. Thus, the methyl carbon signals of interest for the spin diffusion analysis below result purely from three glycolysis amino acids: Leu, Val, and Ala.

Figure 3a,b compares the room-temperature 2D PDS spectra of 1,6-colicin between the soluble and the MB states after a mixing time of 400 ms. It can be seen that many cross-peaks present in the soluble protein spectrum are missing in the membrane protein spectrum. For example, the F/Y δ –L $\delta 1$ /V $\gamma 1$ peak (129.5, 21.4 ppm) and the F/Y β –L $\delta 1$ /V $\gamma 1$ peak (36.2, 21.4 ppm) disappeared in the membrane protein spectrum. The 1D cross sections, taken from the average of the column and row at the corresponding frequencies, are shown for F/Y δ (129.5 ppm), F/Y β (36.2 ppm), and A β (16.0 ppm) (Figure 3d–f). They indicate that the changes in the cross-peak intensities are often an unambiguous yes (for soluble colicin) and no (for MB colicin) situation.

The reduction of cross-peak intensities can result from reduction of the spin diffusion coefficients and/or from distance increases in the MB state. The main factors influencing the diffusion coefficient are ^1H decoupling and motion, since both reduce the ^1H – ^1H and ^1H – ^{13}C dipolar couplings, which in turn affect the overlap between the two ^{13}C single-quantum signals. This overlap is described by the integral $f_{ij}(0) = \int d\omega f_i(\omega)f_j(\omega)$,³⁰ where $f_{i,j}(\omega)$ is the single-quantum spectrum of each peak. A well-known example of motion-facilitated ^{13}C spin diffusion through an increase of the overlap integral is adamantane,³¹ a plastic crystal with large-amplitude motion that permitted the observation of spin diffusion even among ^{13}C sites

at natural abundance. Our previous C–H dipolar coupling measurements showed that MB colicin exhibits amplitude segmental motions larger than those of the soluble state due to thermal motions of the lipid bilayer. The C–H order parameters were 0.88–0.93 for the backbone and 0.60–0.75 for the side chain, which are smaller than the order parameters of 0.97–1.0 for the backbone and 0.87–0.88 for the side chain in the soluble state.³² For ^{13}C chemical shift differences of 2–10 kHz (20–100 ppm), this enhanced although still moderate segmental motion may actually increase the overlap integral and thus facilitate spin diffusion. Indeed, for intraresidue cross-peaks with fixed ^{13}C – ^{13}C distances, the cross-peak intensities are higher in the MB state than those in the soluble state (see below), indicating that the segmental motions of the MB protein increase rather than decrease the ^{13}C diffusion coefficient.

To eliminate the possibilities of other motional factors such as aromatic ring flips complicating the distance analysis, we carried out the 2D ^{13}C spin diffusion experiment for the MB colicin at 243 K, well below the gel-to-liquid crystalline phase transition temperature of the lipids (271 K). The 2D ^{13}C – ^1H LG-CP spectrum of the MB colicin Ia channel domain at 243 K shows dipolar couplings either the same or even slightly larger than those of the soluble protein at room temperature (Supporting Information Figure S2). Thus, direct distance comparison can be made between the membrane protein at 243 K and the soluble protein at room temperature. The low-temperature PDS spectrum of the MB colicin Ia channel domain is shown in Figure 3c. The attenuation of inter-residue cross-peaks persisted at low temperature. Thus, the cross-peak reduction can indeed be attributed to distance increases in the MB protein.

To quantitatively compare the cross-peak intensity buildup between the two states of colicin Ia channel domain, we measured a series of 2D PDS spectra with varying mixing times. The cross-peak intensities, which are the sum of the two symmetric peaks ($I_{AB} + I_{BA}$) in the 2D spectra, were normalized by the total intensity of the four rows and columns that contain the cross-peaks. Two types of buildup behaviors are observed. In the first, the MB protein exhibits no detectable or weak

(30) Meier, B. H. *Adv. Magn. Opt. Reson.* **1994**, *18*, 1–115.

(31) Bronniman, C. E.; Szeverenyi, N. M.; Maciel, G. E. *J. Chem. Phys.* **1983**, *79*, 3694–3700.

(32) Huster, D.; Xiao, L.; Hong, M. *Biochemistry* **2001**, *40*, 7662–7674.

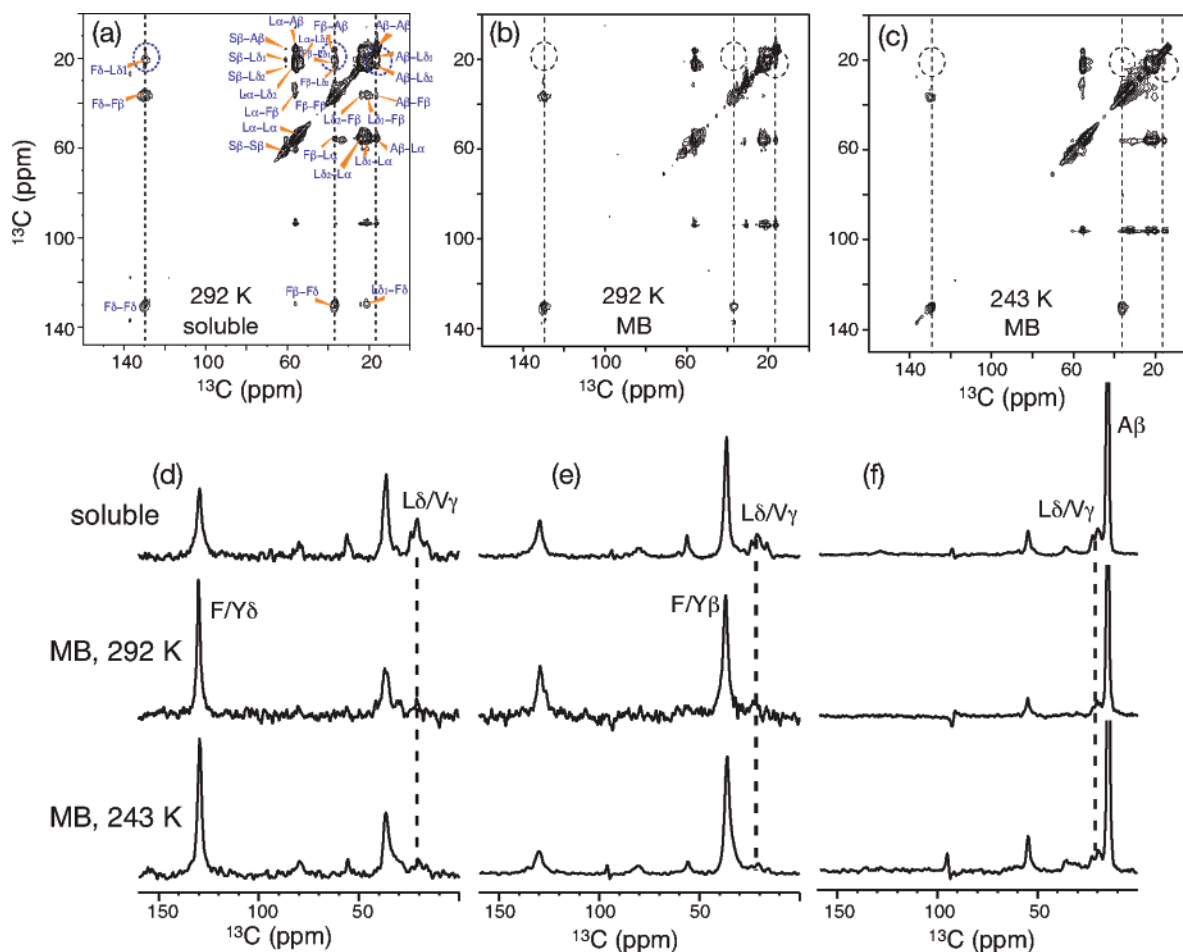


Figure 3. 2D PDSD spectra of 1,6-colicin with a mixing time of 400 ms. (a) Soluble protein, with assignments indicated. (b,c) Membrane-bound (MB) protein at 292 and 243 K. Dashed circles highlight cross-peak intensity differences. (d–f) Selected cross sections from the 2D spectra of the soluble protein (top row), the room-temperature membrane protein (middle row), and the low-temperature membrane protein (bottom row). The cross sections are the average of the corresponding column and row. (d) F/Y δ slice at 129.5 ppm. (e) F/Y β slice at 36.2 ppm. (f) A β slice at 16.0 ppm. Note the significant drop of the cross-peak intensities of the MB protein at both temperatures.

signals for all mixing times up to 500 ms, while the soluble protein shows much higher cross-peaks that increase with the mixing time. This is the case, for example, for F/Y δ –L δ 2 and A β –L δ 2 (Figure 4b,d). The second type of cross-peaks exhibits similar or higher intensities for the MB colicin. This is the case for the A β –L α and F/Y δ –F/Y β peaks (Figure 5). The intraresidue F/Y δ –F/Y β cross-peak provides an important control for assessing the diffusion coefficients of the two states of the protein. This intraresidue F/Y δ –F/Y β cross-peak (Figure 5b) is 5–10 times higher than the interresidue cross-peaks in Figure 4, consistent with the fact that the two-bond distance is fixed at 2.53 Å, much shorter than any potential inter-residue contacts. Because the distance is fixed, any difference in the cross-peak buildup curves between the soluble and MB protein must result from difference in the diffusion coefficients. The MB colicin shows higher F/Y δ –F/Y β intensities for most mixing times, confirming that the enhanced segmental motions of the membrane protein increase the overlap between the ^{13}C single-quantum line shapes. Thus, spin diffusion is actually more efficient in the MB state than in the soluble state, and the reduced cross-peaks of the MB colicin must result from distance increases.

To understand the exact nature of this distance increase, we consider the number of interhelical and intrahelical contacts

within a cutoff distance of 5.5 Å in soluble colicin. For example, 18 F δ –L δ 2 distances within 5.5 Å were found in the soluble protein structure, 15 of which are interhelical while 3 are intrahelical. The statistics are shown in Figures 4 and 5 as bar graphs for each cross-peak. For unresolved peaks such as Phe and Tyr C δ , and L δ 1 and V γ 1, all possible contacts are considered. A distance of 5.5 Å was estimated to be the upper limit detectable by ^{13}C spin diffusion within 500 ms.^{9,33} Increasing the cutoff distance to 7.0 Å did not change the relative weight of the interhelical and intrahelical contacts. Side chain–side chain cross-peaks such as F/Y δ –L δ n and A β –L δ 2 appear to have more interhelical contacts than intrahelical ones, while backbone–side chain cross-peaks such as A β –L α are dominated by intrahelical contacts.

Figures 4 and 5 show a clear correlation between the amount of cross-peak intensity reduction and the percentage of interhelical distances: the larger the fraction of interhelical contacts in the soluble protein, the larger the drop of the cross-peak intensity in the MB state. Since we have previously shown that the helicity of colicin Ia channel domain is not significantly changed by membrane binding,¹⁵ this suggests that the intensity decrease results from an increase of the interhelical distances

(33) Castellani, F.; Rossum, B. J. v.; Diehl, A.; Rehbein, K.; Oschkinat, H. *Biochemistry* **2003**, *42*, 11476–11483.

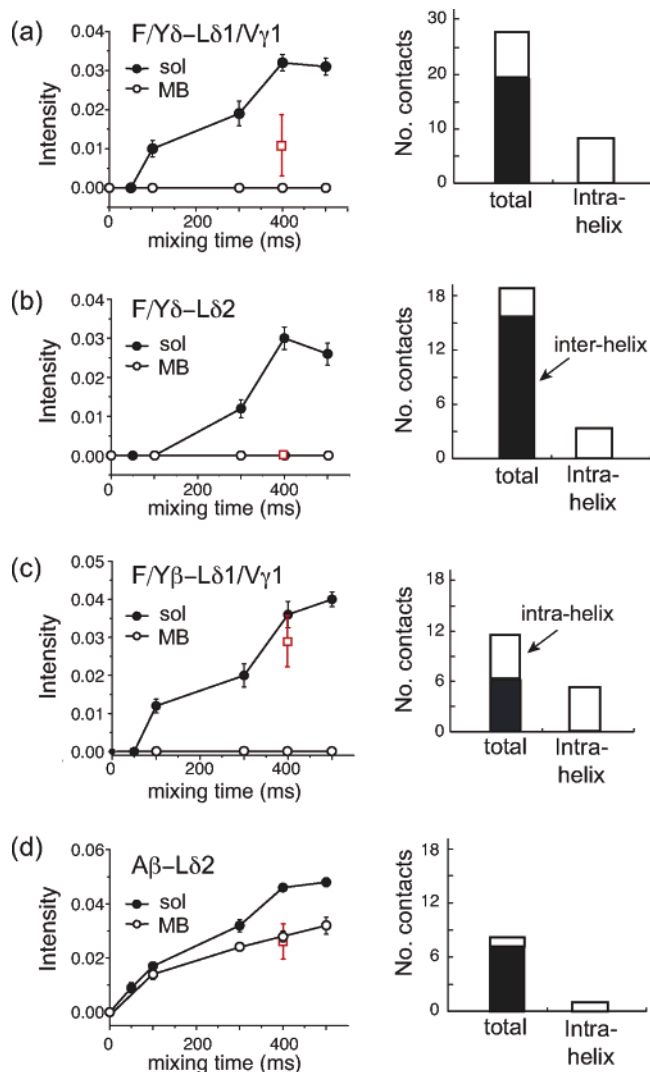


Figure 4. ^{13}C spin diffusion buildup curves for inter-residue cross-peaks (left column) and the corresponding numbers of intrahelical (open) and interhelical (filled) contacts within 5.5 Å in the soluble colicin structure (right column). The cross-peaks are (a) $\text{F/Y}\delta\text{-L}\delta 1/\text{V}\gamma 1$, (b) $\text{F/Y}\delta\text{-L}\delta 2$, (c) $\text{F/Y}\beta\text{-L}\delta 1/\text{V}\gamma 1$, and (d) $\text{A}\beta\text{-L}\delta 2$. Filled circles represent the soluble colicin data at 292 K. Open circles and red open squares represent the MB colicin data at 292 and 243 K, respectively.

after membrane binding. Indeed, for the $\text{A}\beta\text{-L}\alpha$ peak (Figure 5a), which results mostly (11 out of 15) from intrahelical contacts in the soluble protein structure, the buildup curves are similar between the two states, confirming that intrahelical distances are largely unaffected by membrane binding. Combined, these suggest that membrane binding does not change the secondary structure or intrahelical distances of colicin Ia channel domain, but significantly loosens the tertiary structure, lengthening the interhelical distances.

The $\text{A}\beta\text{-L}\delta 2$ cross-peak (Figure 4d) shows a smaller gap between the soluble and the MB states, despite the fact that only one out of eight contacts found within 5.5 Å is intrahelical and should have weakened the signal of the MB protein more substantially. This may result from relayed transfer of the $\text{A}\beta$ magnetization first to $\text{L}\alpha$ and then to $\text{L}\delta 2$. Eleven out of 15 $\text{A}\beta\text{-L}\alpha$ contacts are intrahelical (Figure 5a); thus $\text{A}\beta\text{-L}\delta 2$ diffusion is likely facilitated by this relayed mechanism.

Figures 4 and 5 also show the 400 ms PDSM cross-peak intensities of the MB colicin at 243 K. The most dramatic

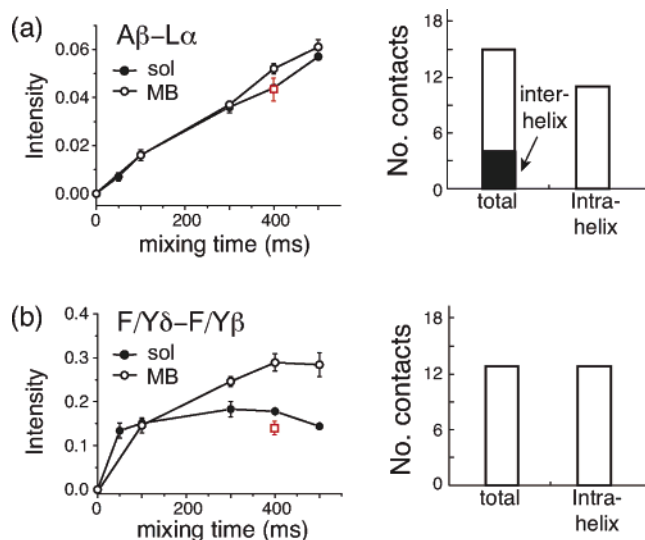


Figure 5. ^{13}C spin diffusion buildup curves (left column) and the numbers of interhelical and intrahelical contacts within 5.5 Å in the soluble colicin structure. (a) $\text{A}\beta\text{-L}\alpha$. (b) $\text{F/Y}\delta\text{-F/Y}\beta$. Symbols are the same as those in Figure 4. At room temperature, the MB protein exhibits similar or faster spin diffusion than the soluble protein due to the predominance of intrahelical contacts and the large diffusion coefficient.

change is seen for the intraresidue $\text{F/Y}\delta\text{-F/Y}\beta$ cross-peak (Figure 5b), which now has an intensity lower than that of the soluble protein, in contrast to the room-temperature result. This further confirms the hypothesis that reduced motion decreases the overlap integral and slows down spin diffusion in the MB colicin. Among the five inter-residue cross-peaks examined, four ($\text{F/Y}\delta\text{-L}\delta 1/\text{V}\gamma 1$, $\text{F/Y}\delta\text{-L}\delta 2$, $\text{A}\beta\text{-L}\delta 2$, $\text{A}\beta\text{-L}\alpha$) are either unaffected or only slightly modified by the temperature change, and the reduction of cross-peak intensity compared to that of the soluble protein is retained. The only significant deviation from the room-temperature data occurred for the $\text{F/Y}\beta\text{-L}\delta 1/\text{V}\gamma 1$ cross-peak (Figure 4c), which increased in intensity but is still lower than the soluble protein data. This is consistent with the fact that $\text{F/Y}\beta\text{-L}\delta 1/\text{V}\gamma 1$ has the largest fraction of intrahelical contacts among the aromatic-methyl cross-peaks (Figure 4a–c), and thus the MB protein retains the largest number of distances within spin diffusion reach.

Overall, the PDSM data indicate that membrane binding increases the interhelical distances while retaining the intrahelical ones. This implies an open and extended structure for the MB colicin Ia channel domain, which is consistent with previous solid-state NMR studies of the secondary structure, dynamics, and topology of colicin Ia channel domain. ^{13}C isotropic and anisotropic chemical shifts of the soluble and MB colicin Ia channel domain do not differ significantly, suggesting that the helicity of the protein is similar between the two states.¹⁵ However, the MB protein exhibits amplitude segmental motions much larger than those of the soluble protein,³² which indicates that the protein adopts a looser tertiary structure upon membrane binding and is able to interact extensively with the lipid molecules. ^1H spin diffusion from lipids and water to protein indicated that a substantial portion of the protein is located at the surface of the bilayer while a small component is deeply embedded in the membrane.^{22,34} These data support an

(34) Kumashiro, K. K.; Schmidt-Rohr, K.; Murphy, O. J.; Ouellette, K. L.; Cramer, W. A.; Thompson, L. K. *J. Am. Chem. Soc.* **1998**, *120*, 5043–5051.

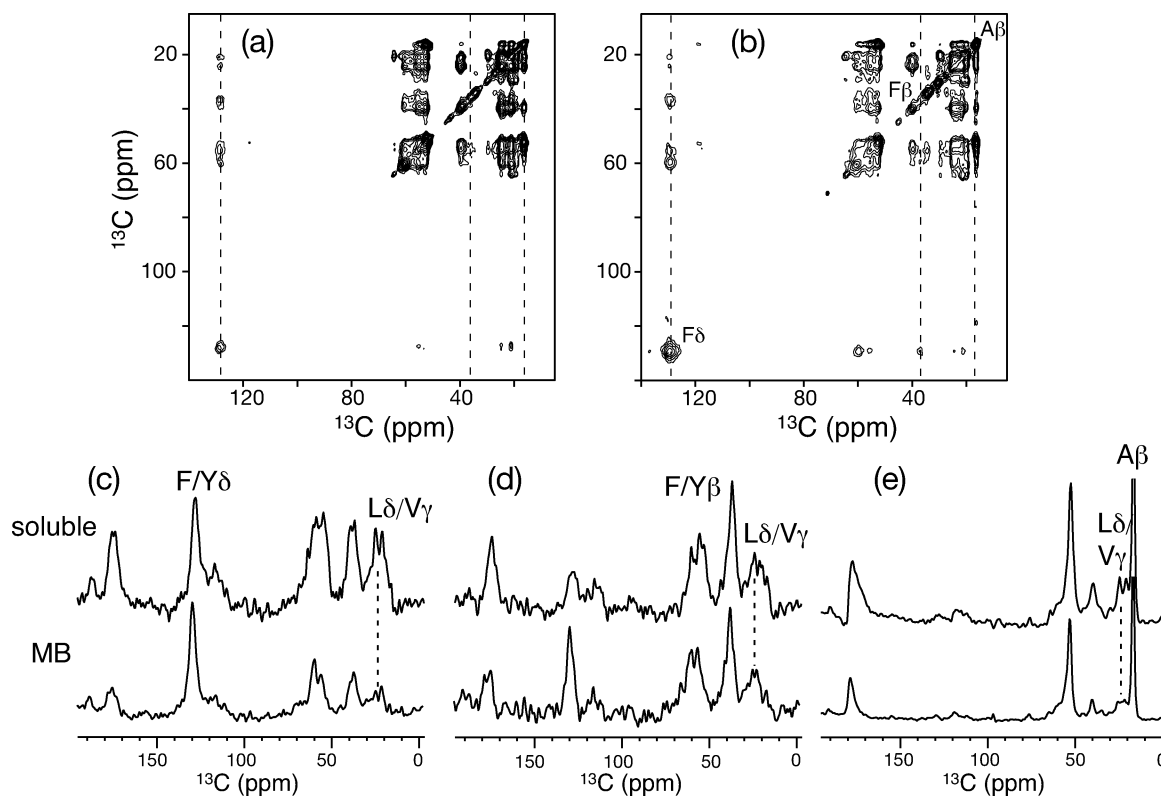


Figure 6. 2D PDSD spectra of pU-colicin in the (a) soluble and (b) MB states at 292 K. Mixing time: 300 ms. (c–e) ω_1 cross sections from the 2D spectra of the soluble (top row) and the MB protein (bottom row). (c) F/Y δ slice at 129.5 ppm. (d) F/Y β slice at 36.2 ppm. (e) A β slice at 16.0 ppm.

“umbrella” model for the MB colicin Ia channel domain.^{20,35} The present ^{13}C spin diffusion data show that the surface of this “umbrella” is extended and possibly away from the hydrophobic “stem”, thus reducing the cross-peak intensities in the spectra.

The different spin diffusion behavior of the soluble and MB colicin persists when partial uniform ^{13}C labeling was used (Figure 6). However, the significant peak overlap makes assignment of inter-residue cross-peaks difficult, thus the simplification offered by 1,6- ^{13}C labeling is crucial for concluding distance elongation in the MB protein.

It is interesting to compare ^{13}C spin diffusion with ^1H spin diffusion, which is far more efficient due to the 16-fold stronger dipolar coupling. ^1H spin diffusion can be detected through ^{13}C , using the CHHC technique developed recently for uniformly ^{13}C -labeled proteins.^{36,37} The ^1H spin diffusion buildup curves for a number of inter-residue cross-peaks in the soluble 1,6-colicin are shown in Supporting Information Figure S3. The cross-peak intensities are either comparable to or higher than the corresponding PDSD cross-peaks; thus in principle ^1H spin diffusion can detect longer distances. However, the sensitivity of CHHC is much lower, as shown by the larger error bars. This is because only 30% of all carbons in colicin Ia channel domain are labeled with the TEASE [1,6- ^{13}C] glucose scheme. Thus, at long ^1H mixing times, $\sim 70\%$ of the ^1H magnetization is transferred to ^1H sites bonded to ^{12}C . Due to this inherent sensitivity limitation, the CHHC technique is not well suited for selectively labeled proteins.

Figure 7a shows the crystal structure of the soluble colicin Ia channel domain (PDB accession code: 1CII) and all F δ –L δ 1 distances within 5.5 Å. A total of 15 distances are found, a subset of those shown in Figure 4a. Figure 7b shows a model of the MB colicin Ia channel domain to illustrate the possible extension of the protein after membrane binding. The model was obtained by modifying the torsion angles of residues in the loops and turns connecting consecutive helices. This produced an extended helical array¹⁶ for helices 1–7, while putting the hydrophobic helices 8 and 9 roughly perpendicular to the rest of the protein. This perpendicular orientation is not determined by the current PDSD experiment, but is derived from solid-state NMR ^1H spin diffusion²² and orientation measurements²³ and from trapping of biotinylated residues by trans-side streptavidin in a planar bilayer.³⁸ The model does not represent the actual 3D structure of the MB protein, which requires many more distance constraints than currently available; however, it illustrates the dramatic distance increase possible without changing a large number of torsion angles from the soluble protein structure. In this extended helical array, 10 of the F δ –L δ 1 distances increased dramatically, to 15–50 Å, while five intrahelical distances remained similar to before. Those residue pairs close to the protein backbone but belonging to a helix and its nearest loops are considered intrahelical to avoid skewing the statistics in favor of the interhelical category. By keeping the intrahelical torsion angles the same as those in the soluble protein, we found that the ratio of the lengthened interhelical distances versus

(35) Parker, M. W.; Postma, J. P. M.; Pattus, F.; Tucker, A. D.; Tsernoglou, D. *J. Mol. Biol.* **1992**, *224*, 639–657.

(36) Lange, A.; Luca, S.; Baldus, M. *J. Am. Chem. Soc.* **2002**, *124*, 9704–9705.

(37) Lange, A.; Seidel, K.; Verdier, L.; Luca, S.; Baldus, M. *J. Am. Chem. Soc.* **2003**, *125*, 12640–12648.

(38) Kienker, P. K.; Qiu, X.; Slatin, S. L.; Finkelstein, A.; Jakes, K. S. *J. Membr. Biol.* **1997**, *157*, 27–37.

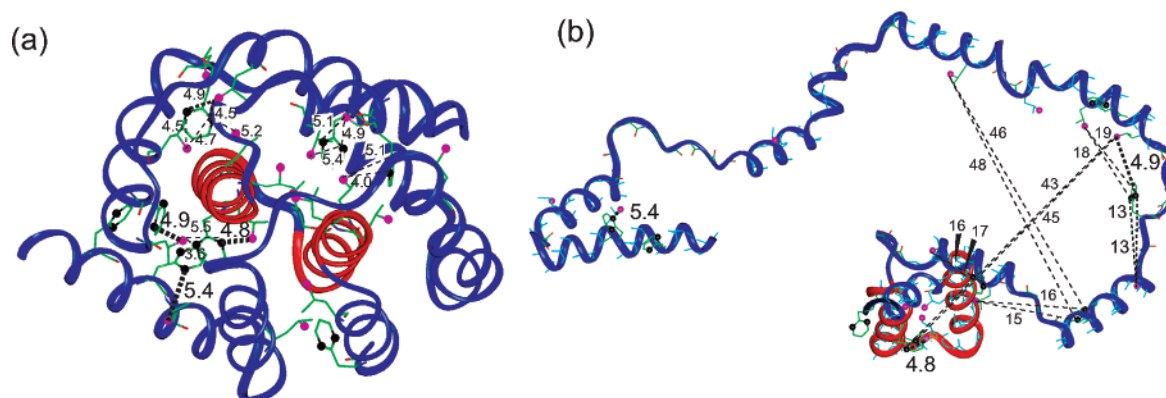


Figure 7. Schematic model of distance elongation and structural rearrangement of colicin Ia channel domain upon membrane binding. (a) Fifteen F δ –L δ 1 contacts within 5.5 Å are found in the soluble structure (PDB code: 1CII). (b) Model of the MB protein, looking down the plane of the bilayer. Only the torsion angles of loop residues are modified. This increased most interhelical distances (in angstroms) to above 15 Å.

unchanged intrahelical distances is relatively independent of the actual torsion angle changes used for the turn and loop residues.

Site-specific distance constraints for MB colicins have been previously obtained using fluorescence resonance energy transfer (FRET) from Trp donors to extrinsic fluorescent probes attached to Cys at specific residues. These experiments found clear evidence of distance elongation upon membrane binding of colicins A and E1.^{16–18} Compared to the present 2D solid-state NMR approach, which gives cross-peaks for only short distance (<5.5 Å) contacts, the FRET method probes much longer distances of 15–35 Å and can be site-specific. However, it has the uncertainties of potential perturbation of the extrinsic probe to the protein structure, significant mobility of the probe, and changes of the energy transfer efficiency by the membrane. EPR spectroscopy has also been used to probe conformational changes of colicin E1 channel domain. By monitoring the mobility changes in the EPR spectra of site-directed nitroxide spin labels as a function of time, we inferred the insertion depths of the labeled residues and the time course of protein binding to the membrane.¹⁹ Again, however, a bulky probe is necessary for this technique. Compared to these two methods, spin diffusion NMR requires no extrinsic probe and thus is less perturbing to the protein. It also allows direct internal calibration of cross-peak intensities for membrane-induced mobility changes. Moreover, by better sample preparation protocols and tailored labeling schemes, it is possible to enhance the spectral resolu-

tion, thus yielding multiple site-specific distance constraints from a single experiment.⁹

In conclusion, the use of sparse side chain ¹³C labeling and ¹H-driven ¹³C spin diffusion unambiguously indicates the lengthening of interhelical distances when colicin Ia channel domain binds to the membrane. The strong attenuation of many inter-residue cross-peaks for the MB sample is well correlated with high percentages of short interhelical contacts in the soluble state, while cross-peaks with similar intensities between the two states have mostly intrahelical contacts. Thus, the MB structure of colicin Ia channel domain may be described as a “molten globule”, in which individual helices retain their structure while the packing of the helices is significantly loosened. Spin diffusion NMR is an excellent way of identifying global structural changes of proteins and is capable of providing long-distance constraints in a qualitative but unambiguous fashion.

Acknowledgment. This work is supported by an NSF CAREER Grant (MCB-0093398) and a Sloan Fellowship to M.H.

Supporting Information Available: ¹³C direct polarization spectrum of 1,6-colicin, 2D LG-CP spectra of soluble and membrane-bound colicin Ia channel domain, and ¹H spin diffusion buildup curves for several inter-residue peaks from the 2D CHHC spectra of soluble 1,6-colicin. This material is available free of charge via the Internet at <http://pubs.acs.org>.

JA0433121